ARTICLES

Synthesis of Axially Substituted Tetrapyrazinoporphyrazinato Metal Complexes for Optical Limiting and Study of Their Photophysical Properties

Danilo Dini,[†] Michael Hanack,*[,†] Hans-Joachim Egelhaaf,[‡] Juan Carlos Sancho-García,[§] and Jerome Cornil[§]

Institutes of Organic Chemistry and Physical and Theoretical Chemistry, University of Tübingen, Auf der Morgenstelle 18, D 72076 Tübingen, Germany, and Laboratory for Chemistry of Novel Materials, Center for Research in Molecular Electronics and Photonics, University of Mons-Hainaut, Place du Parc 20, B-7000 Mons, Belgium

Received: March 20, 2004; In Final Form: January 27, 2005

The synthesis, characterization, and various photophysical properties of axially substituted tetrapyrazinotetraazaporphyrinatotitanium(IV) oxide (Pyz_4TAPTiO) (**1**), tetrapyrazinotetraazaporphyrinatovanadium(IV) oxide (Pyz_4TAPVO) (**2**), tetrapyrazinotetraazaporphyrinatozirconium(IV) dihydroxide [Pyz_4TAPZr$(OH)_2$] (**3**) are reported. Nonlinear optical (NLO) properties of Pyz_4TAPs **1**−**3** have been evaluated at 532 nm with nanosecond pulses for optical limiting (OL). It is found that the introduction of nitrogen atoms in the condensed rings of the tetrapyrrolic macrocycles together with the presence of axial substituents lead to an improvement of the excited-state absorption properties in comparison to phthalocyanines (Pcs). In the linear optical regime Pyz_4-TAPs **1**−**3** display a blue shift (about 50−60 nm) of the main UV−vis absorption bands with respect to Pcs and exhibit orange-red fluorescence, which can be observed with the eye in the case of **1**. Frontier electronic orbitals of a Pyz_4TAP could be depicted from available experimental data and the results of density functional theory (DFT) calculations. In the solid state, Pyz_4TAPTiO (**1**) displays photoconducting properties.

Introduction

Tetrapyrazinotetraazaporphyrin (Pyz_4TAP) is a heteroaromatic analogue of phthalocyanine (Pc) and is characterized by the presence of eight nitrogen atoms occupying the 1, 4, 8, 11, 15, 18, 22, and 25 positions of the conjugated macrocycle, imparting the same symmetry properties of the Pc (Chart 1). The first synthesis of metal Pyz_4TAPs was reported in 1937 by Linstead et al.[1] as an extension of the preparation of Pc analogous. Since then the attention toward these compounds was not as high as toward their aromatic Pc counterparts, despite the strong structural resemblance with Pcs and the likewise ease of preparation.[2] The few reported studies on Pyz_4TAP properties mostly involved the determination of photoconductivity for the development of charge-generating materials (CGMs),[2a,3] whereas substituted R_xPyz_4TAPs have been considered for the realization of discotic meso phases.[4] More recently the nonlinear optical (NLO) properties of some Pyz_4TAPCus have been studied, and interestingly, these materials appeared to be attractive for optical limiting (OL) applications.[5] This first study was focused on the evaluation of OL properties on Pyz_4TAP−metal complexes with a bivalent central metal that do not have additional axial substituents. On the other hand, it was later recognized that the presence of an axial substituent is desirable for the realization of more effective OL materials.[6] For this reason the syntheses of the axially substituted Pyz_4TAPTiO (**1**), Pyz_4TAPVO (**2**),[2h] and Pyz_4TAPZr$(OH)_2$ (**3**) (Figure 1)[7] have been carried out with the aim of evaluating their OL properties in the axially substituted heteroaromatic complexes. In addition to OL investigations, the determination of other photophysical properties of Pyz_4TAP's complexes, namely, linear optical absorption and fluorescence, have been accomplished. Density functional theory (DFT)[8] calculations have been also performed on Pyz_4TAP complexes to rationalize the electronic properties of these complexes in comparison with the Pc counterpart. In the case of Pyz_4TAPTiO (**1**), the photoconductive properties in the solid state also have been studied.

CHART 1

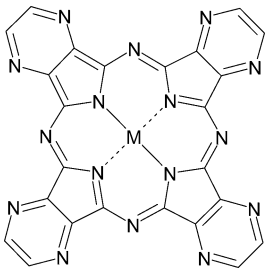

Experimental Section

Synthesis and Characterization. All the synthesized complexes were characterized by cross-polarization magic-angle

* Corresponding author: e-mail hanack@uni-tuebingen.de; fax +49 +-(0)7071 +295268.
[†] Institute of Organic Chemistry University of Tübingen.
[‡] Institute of Physical and Theoretical Chemistry, University of Tübingen.
[§] University of Mons-Hainaut.

10.1021/jp048752t CCC: $30.25
Published on Web 03/04/2005

spinning (CP/MAS) NMR spectroscopy,[9] IR, elemental analysis, and optical spectroscopy. CP-MAS NMR spectroscopy had to be applied due to the general low solubility of the Pyz_4TAP complexes in common organic solvents.[9b]

$Pyz_4TAPTiO$[3d,3e] (**1**) is prepared by heating a mixture of 2,3-pyrazinedicarbonitrile (1.3 g, 1×10^{-2} mol) and titanium(IV) butoxide (1 g, 3×10^{-3} mol) at 130 °C for 6 h. The reaction mixture is washed with hot methanol, filtered, and successively dried under vacuum at 80 °C overnight. The resulting bluish-greenish powder is then heated at 220 °C under vacuum for 16 h. ^{13}C NMR: sharp peak at 148.4 ppm (1×10^3 Hz). CP/MAS ^1H NMR: broad peak centered at 8.0 ppm (1.5×10^3 Hz). MS (MALDI-TOF): 586.5 Da (molecular peak 584.31 Da). IR (in KBr pellet): 3417.93 (br), 3162.17 (br), 2925.95 (sh), 2363.61 (sharp), 2335.89 (sharp), 1671.41 (br), 1624.99 (br), 1534.16 (sh), 1490 (sh), 1390 (sh), 1384.49 (sharp), 1365 (sh), 1285.88 (sh), 1232.54 (sharp), 1157.98 (sh), 1106.21 (sharp), 873.7 (br), 751.54 (br), 708.01 (br), 663.11 (br), 620.62 (sharp). Elemental Analysis Found (Calcd): C, 50.8 (49.4); N, 37.9 (38.5); H, 1.9 (1.5).

Pyz_4TAPVO[2i] (**2**) is prepared by refluxing a solution of 2,3-pyrazinedicarbonitrile (1.3 g, 1×10^{-2} mol) and vanadium(III) chloride (0.6 g, 3.8×10^{-3} mol) in pentanol (2 mL) at 120 °C for 4 h. The solution is filtered and the filtrate is washed with hot methanol. The filtrate is dried under vacuum at 80 °C overnight to remove the solvent. The resulting bluish-greenish powder is then heated at 220 °C under vacuum for 30 h. CP/MAS ^{13}C NMR: due to paramagnetism of the central VO group, the resulting signal could not be recorded. CP/MAS ^1H NMR: very broad peak centered at 8.93 ppm (1.4×10^4 Hz). ESR: at the modulation frequency of 9.4×10^9 Hz and with field amplitude modulation 0.487 G, the derivative signal is centered at 3390 G. MS (MALDI-TOF): 588.6 Da (molecular peak 587.38 Da). IR (in KBr pellet): 3418.00 (br), 3161.25 (br), 2910 (sh), 2362.45 (sharp), 2337.35 (sharp), 1680.96 (br), 1530.81 (br), 1492.36 (br), 1384.44 (sharp), 1363.10 (sharp), 1213.59 (sharp), 1150 (sh), 1095.81 (sharp), 990.44 (br), 915.27 (sharp), 759.22 (sharp), 664.01 (sharp), 620.15 (sharp). Anal. Found (Calcd): C, 51.5 (49.1); N, 37.6 (38.2); H, 2.2 (1.4).

$Pyz_4TAPZr(OH)_2$ (**3**) is prepared by heating a mixture of 2,3-pyrazinedicarbonitrile (1.3 g, 1×10^{-2} mol) and a solution of zirconium(IV) butoxide [80% (w/w) in 1-butanol] (1.5 g) at 110 °C for 2.5 h. CP/MAS ^{13}C NMR: sharp peak at 147.16 ppm and a shoulder at 166.26 ppm (4.5×10^3 Hz). CP/MAS ^1H NMR: broad peak centered at 7.91 ppm (1.4×10^4 Hz). MS (MALDI-TOF): 630.2 Da (molecular peak 645.67). In the case of **3** the detected peak is determined by the removal of one hydroxy group upon protonation of **3** under the experimental conditions of MALDI-TOF technique. Evidences of dimeric species with formula $(Pyz_4TAPZr)_2O_xH_y$ [detected peaks 1242.1 Da (attributed to the dimer with $x = 1$ and $y = 2$) and 1257.5 Da (attributed to the dimer with $x = 2$ and $y = 1$)] could be also found following the protonation of **3** under MALDI-TOF experimental conditions. IR (in KBr pellet): 3165.27 (v br), 2370.61 (br), 1732.23 (br), 1681.54 (br), 1632.61 (br), 1384.46 (sharp), 1211.08 (sharp), 1108.15 (sharp), 746.48 (br), 620.79 (sharp). Anal. Found (Calcd): C, 43.8 (44.7); N, 33.9 (34.7); H, 2.1 (1.6).

Nonlinear Optical Measurements. The nonlinear optical absorption spectra of compounds **1**−**3** in chloroform solutions are measured at the Nd:YAG laser wavelength 532 nm with 5 ns pulses. The OL effect is determined by means of the *Z*-scan technique in the open aperture mode.[10] The transmittance of the sample is recorded as a function of the distance from the focus ($Z = 0$) of a Gaussian beam, at which the incident light intensity is at maximum. The power of a single pulse ranges in the interval $(0.1-2) \times 10^7$ W, whereas the maximum intensity experienced by the sample at the beam focus ranges in the interval $(1-25) \times 10^{12}$ W m^{-2} (beam waist radius is about 5×10^{-4} m). The frequency of sample irradiation is 10 pulses/s and the optics of incidence is f/10. The optical path through the sample is 0.1 cm. The linear transmittance of the Pyz_4TAPMX solutions at $\lambda = 532$ nm ranges in the interval 90−95% with concentration of the active molecules ranging in the interval $(4-8) \times 10^{-5}$ M. The solvent (chloroform) does not show any nonlinear optical effect in the range of light intensities used in this study.

Absorption and Fluorescence Spectra. Optical spectra of **1**, **2**, and **3** in chloroform and pyridine solutions were taken on a UV−vis scanning spectrophotometer (UV-2102 Pc from Shimadzu Scientific). The optical path length of the probing light beam through the quartz cell is 1 cm. Fluorescence spectra from solutions of **1**−**3** were obtained on a SPEX Fluorolog 222 fluorometer.[11a] Fluorescence quantum yields were measured on deaerated solutions, with PcZn as a reference.[11b] Fluorescence lifetimes were measured by the time-correlated single-photon counting method, with a Hamamatsu diode laser ($\lambda = 653$ nm) for excitation. The signals from the laser electronics and from the photomultiplier (R928) were fed into EG&G ORTEC NIM modules (preamplifier, discriminator, delay, and time-to-amplitude converter) for analysis. The fwhm of the instrument response function is $\Delta t = 700$ ps.

Theoretical Analysis. Density functional theory (DFT) proves to be an extremely reliable and useful computational technique for the study of porphyrins, phthalocyanines, and derivatives[8] and constitutes a valid tool complementing the previous computational approaches adopted for the study of this kind of molecules.[12] Here, the geometries of the macrocycle presented in Chart 1 have been optimized by means of the B3PW91 exchange-correlation functional, which combines the Becke exchange[13] with the Perdew-Wang 91 correlation functional[14] in an hybrid fashion.[15] Restricted and unrestricted Kohn−Sham[16] calculations have been performed with the Gaussian98 package[17] for closed- and open-shell systems, respectively. The 6-31G* basis set was consistently employed for vanadyl and titanyl complexes owing to its good balance between accuracy and computational cost. Since a 6-31G* basis set is not available for the Zr atom, the 3-21G basis set was used instead for the description of the $Pyz_4TAPZr(OH)_2$ complex of that element. In the case of the metal-free porphyrin, the use of a DFT approach is validated by the excellent agreement found between the experimental bond lengths and bond angles and the corresponding calculated values.[18]

The similarity of the ring geometries in metal-free and metalloporphyrinato complexes[19] suggests that the presence of a coordinating central atom other than hydrogen has relatively little impact on the overall shape of the macrocycle.[20] We calculate a slight deviation from planarity for the rings of the TiO and VO complexes, which is driven by steric effects. We have further characterized the nature of the lowest excited states of TiO and VO complexes by using the spectroscopic version[21] of the semiempirical Hartree−Fock INDO method;[22] the latter was successfully exploited in a previous study of the optical properties of porphyrins and related compounds.[23] All the singly excited configurations created by promoting an electron from one of the 40 highest occupied levels to one of the 40 lowest unoccupied levels have been included in the calculations. In view of the experimental data, similar trends are expected for

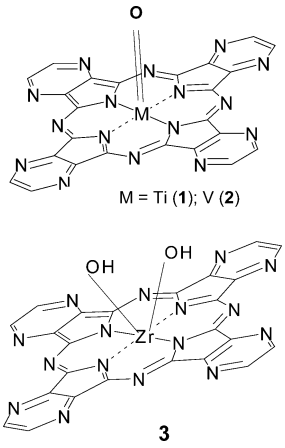

Figure 1. Metallotetrapyrazinotetraazaporphyrins Pyz_4TAPMX with MX = TiO (**1**), VO (**2**), and $Zr(OH)_2$ (**3**).

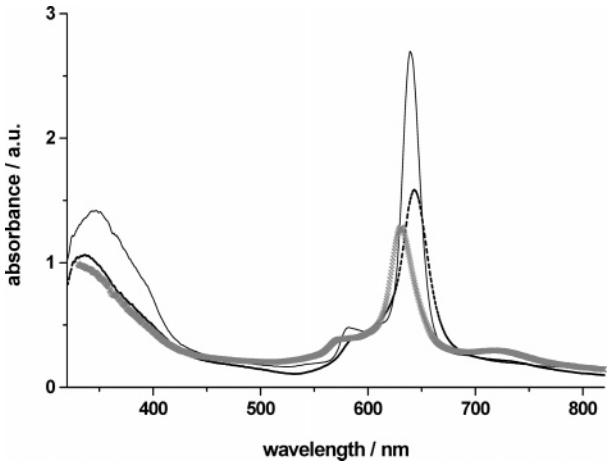

Figure 2. UV−Vis spectra of (dotted line) $Pyz_4TAPTiO$ (**1**), (thin black line) Pyz_4TAPVO (**2**), and (thick gray line) $Pyz_4TAPZr(OH)_2$ (**3**) in pyridine at equal nominal concentrations (2×10^{-5} M).

the zirconium derivative $Pyz_4TAPZr(OH)_2$ that we cannot tackle at the INDO level due to the lack of parametrization for the Zr atom.

Photocurrent Measurements. Thin films of the compounds are deposited onto Pt/sapphire interdigitated electrodes (electrode spacing 100 μm) either by vapor deposition under high vacuum (for phthalocyanines) or by solvent (chloroform) evaporation[24] from the solution of **1**−**3**. The thickness of the films is below 100 nm as monitored with a quartz-crystal microbalance and by means of optical absorption determinations.[25] The applied voltage for the generation of detectable currents through the thin film samples is 60 V. At this value of applied potential, the electrical currents are on the order of 10^{-10}−10^{-9} A as measured with a Keithley 487 picoammeter. In the determination of photoconductivity, the samples are irradiated with a 450-W Xe lamp with the light passing through a Zeiss prism double monochromator.[26]

Results and Discussion

Linear Optical Properties. The linear optical spectra of solutions of $Pyz_4TAPTiO$ (**1**), Pyz_4TAPVO (**2**), and $Pyz_4TAPZr(OH)_2$ (**3**) in pyridine are shown in Figure 2. The maxima of the Q-bands of **1**, **2**, and **3** are observed at 643, 640, and 631 nm, respectively, with vibronic replica [and possibly contributions of ligand-to-metal charge-transfer/metal-to-ligand charge-transfer (LMCT/MLCT) transitions[27]] at 584, 582, and 572 nm, respectively. The comparison of the absorption spectra of Pyz_4TAPs differing by the nature of the central atom−axial ligand combination shows that the main absorptions of $Pyz_4TAPTiO$ (**1**) and Pyz_4TAPVO (**2**) are located approximately at the same wavelengths, whereas the Q-band of $Pyz_4TAPZr(OH)_2$ (**3**) is slightly blue-shifted with respect to those of **1** and **2**. The B bands are centered at 337, 346, and 330 nm for **1**, **2**, and **3**, respectively. An additional band appears in the spectra of **1**−**3** at approximately 720 nm, and this band is most pronounced for $Pyz_4TAPZr(OH)_2$ (**3**). The presence of additional absorption bands at wavelengths longer than that of the Q-band is indicative of aggregation phenomena, especially for $Pyz_4TAPTiO$ (**1**) and $Pyz_4TAPZr(OH)_2$ (**3**) (Figure 3).[28] Moreover, the main absorptions of Pyz_4TAPs appear generally broader than the respective absorptions of Pcs, mainly for the same reason.[29] The analysis of optical spectra thus indicates a higher tendency of Pyz_4TAPs toward molecular aggregation in solution when compared to analogous Pcs. Such a finding is rationalized in terms of additional intermolecular dipole−dipole interactions for Pyz_4TAPs with respect to Pcs.[2i] This is due to the presence of the more electronegative nitrogen atoms in the condensed rings (Figure 1), which impart a prevalent local dipolar character to the C−N bonds present in the pyrazine moieties.[30] In the case of $Pyz_4TAPZr(OH)_2$ (**3**) complex, the axial hydroxy groups can give rise to aggregated entities held together by axial hydrogen bonds. Spectra of **1**−**3** taken in chloroform (not shown here) display broader absorption bands, but the location of the main peaks is almost unchanged with respect to the spectra of **1**−**3** taken in pyridine (Figure 2).

In Figure 3 the absorption spectra of the Pyz_4TAPs are compared to those of their phthalocyanine analogues. The maximum of the Q-band of $Pyz_4TAPTiO$ (**1**) ($\lambda_{max} = 691$ nm) is blue-shifted by about 50 nm ($\Delta E = 0.14$ eV) with respect to the analogous band of PcTiO (**4**). The spectral position of the B band of **1**, which is centered at 345 nm, remains almost unchanged with respect to the analogous band of **4**. Similar differences can be found by comparing the optical spectra of Pyz_4TAPVO (**2**) with PcVO (**5**) (Figure 3b) and $Pyz_4TAPZr(OH)_2$ (**3**) with $PcZr(OH)_2$ (**6**) (not shown).

The fluorescence spectra of $Pyz_4TAPTiO$ (**1**) and PcTiO (**4**) in chloroform are displayed in Figure 4. They exhibit maxima at 649 and 699 nm ($\Delta E = 0.14$ eV), respectively. Hence, the fluorescence maxima of the Pyz_4TAP compounds show the same kind of spectral shifts with respect to the phthalocyanine analogues as well as the absorption maxima. The presence of heteroatoms in the conjugated macrocycle does not alter qualitatively the fluorescence spectra of Pyz_4TAPs with respect to Pcs since a mirror image between the fluorescence (Figure 4) and the absorption curves (Figure 3a) is found in both $Pyz_4TAPTiO$ (**1**) and PcTiO (**4**).[28a,31] As in Pcs, the fluorescence of Pyz_4TAPs is emitted from the S_1 state, which is the final state of the Q absorption band.[28a,32] This leads to the mirror image of fluorescence and absorption spectra, which includes the vibronic sidebands due to macrocycle breathing and CN-stretch vibrations. A small Stokes shift is observed for both **1** (6 nm) and **4** (8 nm), yielding large overlaps between the fluorescence and absorption spectra.[28a]

Quantum Chemical Calculations. The relative energy values and the shape of the frontier molecular orbitals in PcTiO (**4**) and $Pyz_4TAPTiO$ (**1**) are shown in Figure 5. We describe here only the orbitals involved in the electronic transitions associated with the Q and B bands. In both PcTiO (**4**) and $Pyz_4TAPTiO$ (**1**) the lowest two unoccupied orbitals (LUMO and LUMO + 1) are degenerate π-levels extended along the *x* and *y* axes, respectively. The HOMO orbital is spread out over the whole

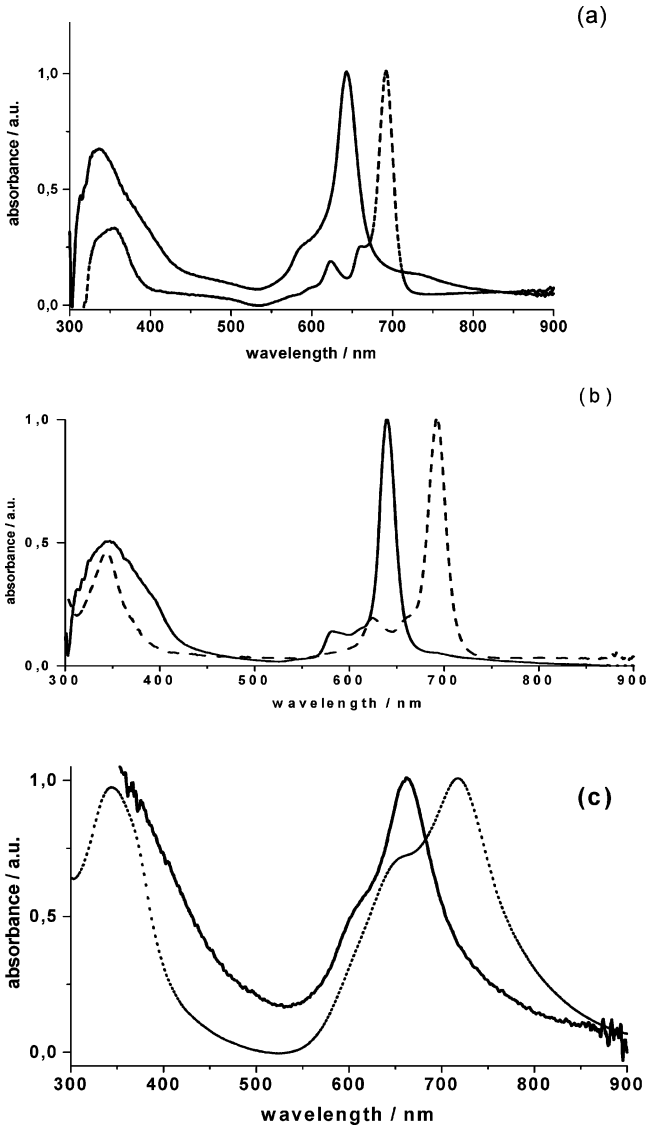

Figure 3. (a) Comparison of normalized UV−vis spectra of Pyz_4-TAPTiO (**1**) (—) and PcTiO (**4**) (---) in pyridine; (b) comparison of normalized UV−vis spectra of Pyz_4TAPVO (**2**) (—) and PcVO (**5**) (---) in pyridine; and (c) comparison of normalized UV−vis spectra of Pyz_4-TAPTiO (**1**) (—) and PcTiO (**4**) (···) thin films (the substrate was glass).

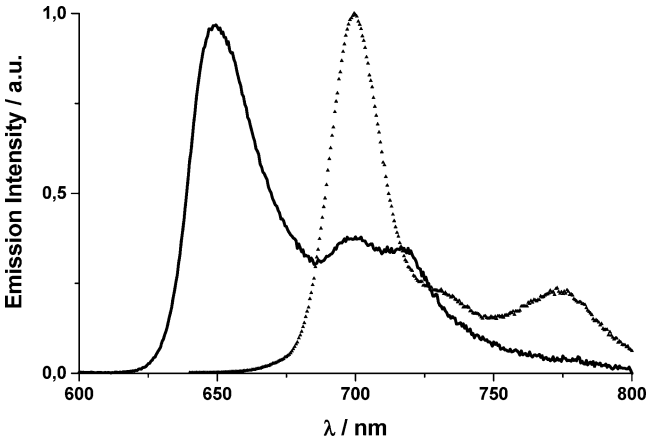

Figure 4. Comparison of the fluorescence spectra of Pyz_4TAPTiO (**1,** —) and PcTiO (**4**, ▲) in chloroform. Samples were irradiated at the wavelengths corresponding to the maxima of absorption of the respective B bands. Solution concentrations were 3×10^{-5} M.

molecular backbone of **1** and **4** and displays nodes at the meso positions of the inner ring. Due to the higher electronegativity of nitrogen with respect to carbon, the frontier molecular orbitals are stabilized when going from PcTiO (**4**) to Pyz_4TAPTiO (**1**) (the same evolution is also observed for conjugated linear rods).[33] The HOMO is stabilized by 0.95 eV while the LUMO is stabilized by only 0.74 eV This difference is due to the larger contributions of the atomic orbitals to the HOMO at the positions where the peripheral N-atoms are located in the Pyz_4TAP compounds. The asymmetry of stabilization increases the HOMO/LUMO gap in Pyz_4TAPTiO (**1**). In contrast, the HOMO − 1/LUMO gap in PcTiO (**4**) (which primarily determines the energy of the B band) is unaltered with respect to the corresponding gap between the HOMO − 5 and LUMO levels in Pyz_4TAPTiO (**1**). Similar trends are also found in the case of Pyz_4TAPVO (**2**) and $Pyz_4TAPZr(OH)_2$ (**3**).

The experimental optical spectra in Figure 3a are readily understood from the changes calculated in the electronic structure when going from PcTiO (**4**) to Pyz_4TAPTiO (**1**) (Figure 5). The Q-band absorption of these molecules, which originates from a transition between the HOMO and the doubly degenerate LUMO levels,[27a,34,35] is blue-shifted by about 0.14 eV upon introduction of the nitrogen atoms in the macroring structure, in good accordance with the calculated increase of the HOMO/LUMO gap of 0.1 eV. Similarly, a blue shift of about 0.1 eV is calculated for the Q-band when going from PcVO (**5**) to Pyz_4TAPVO (**2**), thus reproducing the observed spectral features of **2** (Figure 3b). In contrast, the B-band originating mostly from an electronic transition between the doubly degenerate LUMO levels and the HOMO − 1 and HOMO − 5 levels for PcTiO (**4**) and Pyz_4TAPTiO (**1**), respectively, is located almost at the same energy in both **4** and **1** (Figure 3), as expected from the unaltered HOMO − 1/LUMO gap.

Optical Limiting. The OL produced by the series of compounds **1**−**4** in chloroform solutions with nanosecond pulses at 532 nm is presented in Figure 6. In the analysis of the OL effects, the comparison of the different *Z*-scan profiles is based mainly on the minimum value of normalized transmittance T/T_0 in correspondence to the beam focus ($Z = 0$), the linear transmittance T_0 being the same for all the examined samples (Table 1). At the focus of the Gaussian beam, the intensity I of the beam reaches the maximum value given by the following I vs Z relationship:[10a]

$$I(Z) = E/[\tau w^2(Z)\pi] \qquad (1)$$

where E, τ, and $w(Z)$ are the pulse energy, the pulse duration, and the beam radius as a function of the distance Z from the focus, respectively. The value of T/T_0 at $Z = 0$ grows in the sequence $T/T_0(\mathbf{2})_{Z=0} \approx T/T_0(\mathbf{1})_{Z=0} < T/T_0(\mathbf{3})_{Z=0} \approx T/T_0(\mathbf{4})_{Z=0}$, thus indicating that Pyz_4TAPTiO (**1**) and Pyz_4TAPVO (**2**) are better optical limiters than $Pyz_4TAPZr(OH)_2$ (**3**) and PcTiO (**4**). The incident energy in these experiments is on the order of 100 nJ. The main difference between the *Z*-scan profiles of **1** and **2** is the wider range of optical nonlinearity of **2** with respect to **1** (Figure 6).

The direct comparison of the OL effect produced by the heteroaromatic Pyz_4TAPTiO (**1**) and its aromatic counterpart PcTiO (**4**) shows that the presence of nitrogen atoms in the skeleton of the conjugated network changes considerably the OL properties of the resulting macrocycle−metal complex, leading to a 10% decrease of the minimum value of T/T_0 (Figure 6). Comparison of the nonlinear absorption profiles of Pyz_4TAPTiO (**1**), Pyz_4TAPVO (**2**), and $Pyz_4TAPZr(OH)_2$ (**3**) (Figure 6) indicates that the profiles of **1** and **2** reach approximately the same minimum transmission value in cor-

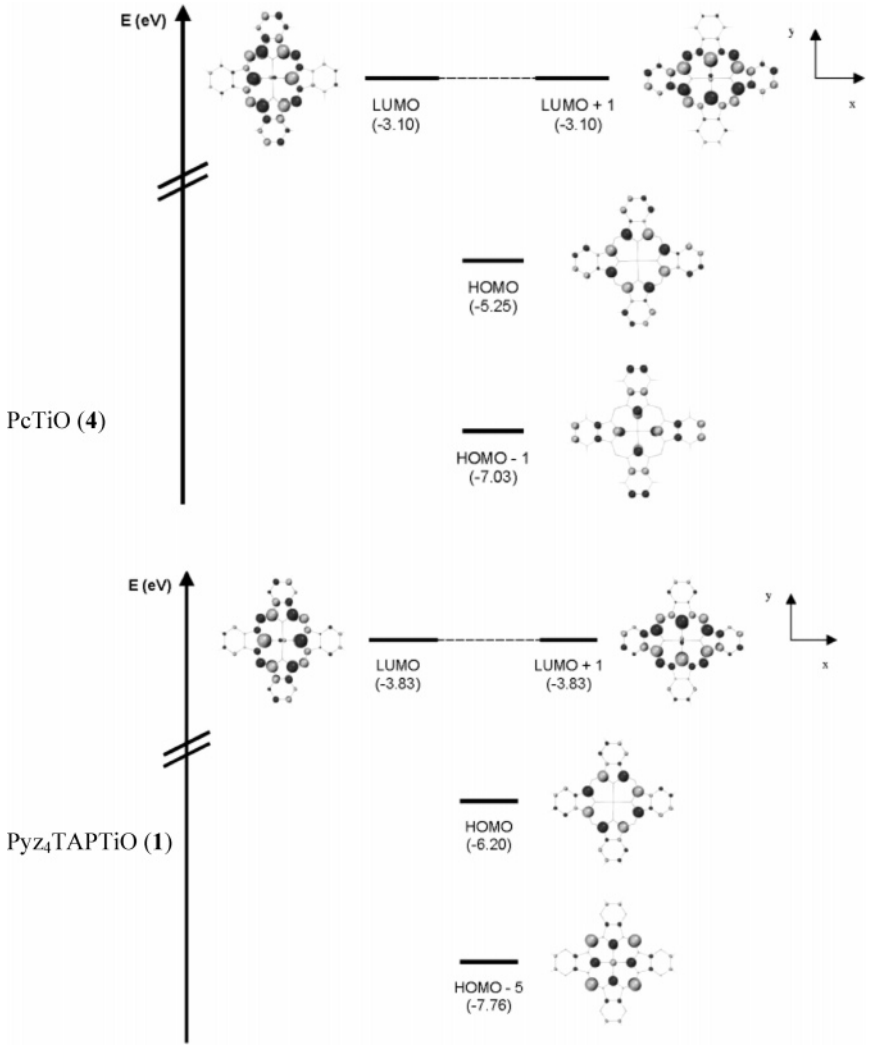

Figure 5. Energies and shapes of the molecular orbitals of PcTiO (**1**) and $Pyz_4TAPTiO$ (**4**); the size and shading intensity of the circles describe the amplitude and the sign of the LCAO (linear combination of atomic orbitals) coefficients associated with the π-atomic orbitals.

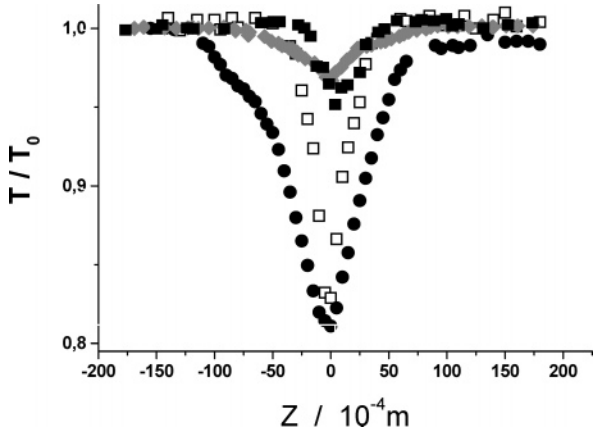

Figure 6. Comparison of the *Z*-scan profiles of (□) $Pyz_4TAPTiO$ (**1**), (●) Pyz_4TAPVO (**2**), (gray diamonds) $Pyz_4TAPZr(OH)_2$ (**3**), and (■) PcTiO (**4**) in chloroform solution. *Z* represents the distance from the beam focus; (T/T_0) represents the normalized transmittance (linear transmittance $T_0 = 90\%$).

respondence of the beam focus position, with Pyz_4TAPVO (**2**) having the largest range of nonlinear optical absorption. In contrast to $Pyz_4TAPTiO$ (**1**) and Pyz_4TAPVO (**2**), the nonlinear absorption of $Pyz_4TAPZr(OH)_2$ (**3**) produces a relatively poor OL effect. This is most likely due to the occurrence of molecular aggregation in solution, as suggested by the analysis of the linear optical spectrum of **3** (Figure 2), which reduces the lifetime of the excited state responsible for the absorption of the second photon[36] and probably diminishes the absorptive properties of the aggregate in the excited state.

TABLE 1: Experimental Conditions Adopted for the Determination of the OL Effect[a]

compd	$C/10^{-5}$ M	T_0 ($\lambda = 532$ nm)	T/T_0 ($Z = 0$) ($\lambda = 532$ nm)
1	4.0	0.90	0.85
2	5.0	0.90	0.80
3	4.0	0.90	0.95
4	4.5	0.90	0.95

[a] C represents the concentration in chloroform solution of the active species $Pyz_4TAPTiO$ (**1**), Pyz_4TAPVO (**2**), $Pyz_4TAPZr(OH)_2$ (**3**) and PcTiO (**4**). T_0 is the linear transmittance of the solution at 532 nm, and T/T_0 ($Z = 0$) is the normalized transmittance of the solution at the beam focus ($Z = 0$) at 532 nm.

When the *Z*-scan profiles of $Pyz_4TAPTiO$ (**1**) and PcTiO (**4**) (Figure 6) are compared, the enhancement of the OL effect associated with the introduction of nitrogen atoms in the condensed conjugated system is quite evident. The presence of nitrogen atoms in Pyz_4TAPs can be considered as the replacement of carbon atoms of the condensed ring by more electron-withdrawing groups. The introduction of pyrazine leads to an increase of the oxidation potential of the conjugated molecule, as confirmed by quantum-mechanical calculations (Figure 5); as a consequence, this improves the chemical stability of

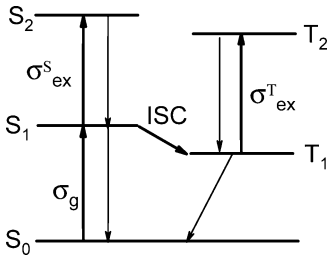

Figure 7. Jablonski diagram for the description of the mechanism of reverse saturable absorption (RSA) upon short-pulse irradiation of chromophores such as phthalocyanines in the visible spectrum. S_0, $S_{1(2)}$, and $T_{1(2)}$ indicate the ground singlet state, the first (second) excited singlet state, and the first (second) excited triplet state, respectively. The chromophore absorbs the first photon through the transition [$S_0 \rightarrow S_1$] and, depending on the dynamics of the irradiated system, will absorb sequentially a second photon through either [$S_1 \rightarrow S_2$] or [$T_1 \rightarrow T_2$] transition. $\sigma_{ex}^{S(T)}$ and σ_g are the absorption cross-sections from the excited singlet (triplet) state and the ground state, respectively. Verification of RSA implies that $\sigma_{ex}^{S(T)} > \sigma_g$. Oblique and straight downward arrows indicate phosphorescence and fluorescence decays, respectively. ISC indicates intersystem crossing [$S_1 \rightarrow T_1$]. For the sake of clarity, only the fundamental vibrational level of the various electronic levels is indicated.

Pyz_4TAPs against oxidation. On the other hand, the strong enhancement of the nonlinear absorption in passing from Pc to Pyz_4TAP solutions (Figure 6) can be attributed to the influence of the heteroatoms on the electronic polarizability of the conjugated molecule (nonresonant dynamic effect), and, more importantly, to the alteration of the excited-state spectrum of the Pyz_4TAPs (molecular resonant effect). In general, both these effects can be involved in the mechanism of nonlinear optical absorption.[36]

At low-intensity irradiation, Pyz_4TAPs show little absorption at 532 nm, 90−95% of the incident light being transmitted at this wavelength. After excitation of the metal complexes into the S_1 state, the excited singlet state decays by return to the ground state [$S_1 \rightarrow S_0$] and by intersystem crossing to the triplet manifold [$S_1 \rightarrow T_1$].[37] Due to the long lifetime of the triplet state, its population grows with increasing light intensities. As the extinction coefficient of triplet−triplet absorption [$T_1 \rightarrow T_n$] at 532 nm exceeds that of ground-state absorption at the same wavelength, an optical limiting effect is observed at sufficiently high intensities.[6a,b,38,39] This means that for all complexes **1**−**3** the occurrence of such nonlinear optical phenomena at 532 nm is due to a mechanism of sequential two-photon absorption (Figure 7). In macrocyclic complexes such as Pcs, Pyz_4TAPs, and analogues it is well established that the effect of reverse saturable absorption[40] can be enhanced either by increasing the absorption cross-section of the excited state [e.g., by shifting the excited-state spectrum relative to the [$T_1 \rightarrow T_2$] transition (Figure 7)] or by accelerating the intersystem crossing (ISC) process that populates the absorbing excited state and, consequently, reduces the probability of occurrence for the deactivation process [$S_1 \rightarrow S_0$], either radiative (fluorescence) or nonradiative (Figure 7). It is found that the photophysical properties of Pyz_4TAPTiO (**1**) are similar to those of PcTiO (**4**). Both titanyl complexes show strong fluorescence and have fluorescence lifetimes on the order of several nanoseconds. In the case of PcTiO a fluorescence quantum yield of $\Phi_F = 0.26$ and a fluorescence lifetime of $\tau_F = 5.3$ ns have been determined in pyridine, yielding a radiative rate constant of $k_F = 4.9 \times 10^7$ s^{-1}. This implies that the differences in OL behavior between complexes **1** and **4** are mostly due to the electronic effects associated with the presence of eight nitrogen atoms and not to kinetic effects in the mechanism of sequential two-photon absorption. This occurs also when Pyz_4TAPVO (**2**) and PcVO (**5**) are compared, but in the case of vanadyl complexes the fluorescence quantum yields are much lower ($\Phi_F < 10^{-3}$), due to the open-shell configuration of the vanadyl moiety (paramagnetism),[11b] which leads to rapid ISC (Figure 7). Thus, the rate constant of intersystem crossing is much faster than the radiative rate constant ($k_{ISC} \gg k_F$) in vanadyl complexes, whereas k_{ISC} is on the same order of magnitude as the radiative rate constant k_F in titanyl complexes. This explains the fact that the triplet state is populated much more efficiently in vanadyl complexes than in titanyl complexes. As a consequence of that, the intensity required for the onset of nonlinear optical behavior due to the absorption of the excited triplet state is lower in vanadyl complexes with respect to titanyl complexes (Figure 6).

Similar to Pcs, the most probable kind of electronic transition in the excited state of axially substituted Pyz_4TAPs at 532 nm is also associated with a partial transfer of electronic charge from the periphery toward the center of the macrocyclic complex.[6e,27] In such conditions, the verification of larger decreases of Pyz_4TAP solution transmittance in the nonlinear optical regime can be ascribed to a larger variation of the transition dipole moment[41] of Pyz_4TAPs with respect to Pcs in the excited state when such a partial charge-transfer process takes place. In the electronic transition involving the excited state of Pyz_4-TAPs, the actual displacement of the electronic charge from the periphery toward the center of the conjugated macrocycle provokes a more dramatic redistribution of the electronic cloud when the conjugated macrocycle comprises electron-withdrawing atoms, like N in the present case, or electron-withdrawing substituents, for example, F or CF_3.[6d,42] This is explained by the fact that electron-withdrawing atoms (or groups) located on the rings conjugated with the tetrapyrrolic core hold a larger portion of the negative charge of the ring further from the tetrapyrrolic core coordinated by the central metal.

Photoconductive Properties of Oxo−titanium(IV) Complexes. In air, at room temperature, the application of a voltage $E = 60$ V produces dark current values i_d on the order of 10^{-9} A for Pyz_4TAPTiO (**1**) and PcTiO (**4**) thin films. It is known that photoconductivity of **4** (and presumably of **1**, as well) is sensitive to the molecular arrangement of the molecules in the solid phase.[43] As partially verified by the presence of quite broad signals in the solid-state CP-MAS ^{13}C and ^1H NMR spectra of **1** and **4** (not reported here) at room temperature, and the scarce solubility of **1** in chloroform, it is expected that Pyz_4TAPTiO thin films obtained from solution casting with chloroform as carrying solvent are probably in an amorphous state. Same considerations are valid for **4** synthesized and deposited with an analogous procedure.[24] The presumed existence of disordered and amorphous states for both **1** and **4** in the configuration of thin films examined here enabled us to ascribe their observed differences in photoconductivity mainly in terms of single-molecule properties rather than in terms of their molecular arrangement in the condensed phase.

The optical spectra of **1** and **4** thin films are given in Figure 3c. PcTiO (**4**) displays a higher value of i_d with respect to Pyz_4TAPTiO (**1**) (1.10×10^{-9} vs 0.50×10^{-9} A). The irradiation of **1** and **4** thin films with light intensity $I_{irr} = 5 \times 10^{-9}$ einstein cm^{-2} s^{-1} at the center of the Q-band at 664 and 715 nm, respectively (Figure 3c), increases the current by 150% for PcTiO (**4**) and only 5% for Pyz_4TAPTiO (**1**). In the adopted thin-layer configuration the photocurrents produced by **1** and **4** displayed ohmic behavior[44] within the potential range $30 < E < 90$ V. The increase of electrical current upon irradiation of Pyz_4TAPTiO (**1**) and PcTiO (**4**) thin films in correspondence

with their Q-band absorption is much larger for **4** than **1** in ambient atmosphere. Such a finding implies a more effective and probably faster photoinduced charge separation in PcTiO (**4**) with respect to Pyz_4TAPTiO (**1**) thin films. Under these conditions molecular oxygen from atmosphere can also participate in the formation of the actual photogenerated carriers in both **1** and **4**.[45] This is consistent with the verification of a lower energy (higher stability) for the HOMO of Pyz_4TAPTiO with respect to PcTiO (Figures 3a and 5).[26a] In fact, the HOMO of these complexes represents the starting electronic orbital in the transition, which leads to charge photogeneration at the exciting wavelength of Q-band.[46] In terms of photocurrent response, the behavior of **1** resembles that of a fluorinated PcTiO in which the presence of the electron-withdrawing fluorine substituents decreases the yield of charge-generating excited species formation due to the stabilization of the HOMO level (thermodynamic effect) and reduces the efficiency of charge separation upon irradiation (trapping effect).[26a,47]

Conclusions

In the present work, the optical limiting properties of the axially substituted complexes of tetrapyrazinotetraazaporphyrinato (Pyz_4TAP) with titanium(IV) oxide (**1**), vanadium(IV) oxide (**2**), and zirconium(IV) dihydroxide (**3**) are reported. Axial substitution in the tetravalent metal complexes together with the presence of nitrogen in the condensed rings of the macrocyclic ligand improves the optical limiting (OL) effect in the visible range when compared to analogous phthalocyanines under similar experimental conditions. Such an improvement is tentatively ascribed to the larger variations of the transition dipole moment in the excited-state transition starting from a triplet excited state. Other alterations of the photophysical properties induced by the replacement of eight carbon atoms with an equal number of nitrogen atoms in the 1, 4, 8, 11, 15, 18, 22, and 25 positions of **1**−**3** are (i) a blue shift of the main UV−vis absorption bands from both solution and solid state with respect to analogous phthalocyanines; (ii) a blue shift of the fluorescence signal from solution with respect to analogous phthalocyanines and the observation of orange-red fluorescence with the eye, and (iii) a decrease of the efficiency of charge photogeneration for **1** in the solid state with respect to its phthalocyanine counterpart. These comparative findings have been rationalized by quantum-mechanical calculations. Through the adoption of density functional theory it was demonstrated that the observed changes of the various photophysical properties in Pyz_4TAP complexes **1**−**3** can be reconducted to the stabilization of their HOMO energy level with respect to phthalocyanines.

Acknowledgment. We are grateful to Dr. James S. Shirk from Optical Sciences Division at the Naval Research Laboratory (Washington, DC) and Dr. G. Y. Yang from DSO National Laboratories (Singapore) for profitable discussions. We also thank Professor W. Blau from Department of Physics at Trinity College (Dublin, Ireland) for having offered the equipment for optical limiting experiments. Mrs. Schindler is kindly acknowledged for the realization of NMR and ESR spectra. For the realization of the work in Tübingen, the financial support from the European Community (Contract HPRN-CT-2000-00020) is gratefully acknowledged. The work in Mons has been partly supported by the Belgian Federal Government "Service des Affaires Scientifiques, Techniques et Culturelles (SSTC)" in the framework of the "Pôle d'Attraction Interuniversitaire en Chimie Supramoléculaire et Catalyze Supramoléculaire (PAI 5/3)", by the Belgian National Fund for Scientific Research (FNRS/FRFC), and by the European Community project NANOCHANNEL (Contract HPRN-CT-2002-00323). J.C. is an FNRS research associate.

References and Notes

(1) Linstead, R. P.; Noble, E. G.; Wright, J. M. *J. Chem. Soc.* **1937**, 911−921.

(2) (a) Danzig, M. J.; Liang, C. Y.; Passaglia, E. *J. Am. Chem. Soc.* **1963**, *85*, 668−671. (b) Kasuga, K.; Nishikori, K.; Mihara, T.; Handa, M.; Sogabe, K.; Isa, K. *Inorg. Chim. Acta* **1990**, *174*, 153−154. (c) Takahashi, K.; Aoki, Y.; Sugitani, T.; Moriyama, F.; Tomita, Y.; Handa, M.; Kasuga, K. *Inorg. Chim. Acta* **1992**, *201*, 247−249. (d) Kobayashi, N.; Rizhen, J.; Nakajima, S.; Osa, T.; Hino, H. *Chem. Lett.* **1993**, 185−188. (e) Kleinwachter, J.; Subramanian, L. R.; Hanack, M. *J. Porphyrins Phthalocyanines* **2000**, *4*, 498−504; (f) Gal'pern, E. G.; Luk'yanets, E. A.; Gal'pern, M. G. *Izv. Akad. Nauk SSSR, Ser. Khim.* **1973**, 1976−1980. (g) Gal'pern, M. G.; Luk'yanets, E. A. *Khim. Get. Soed.* **1972**, 858−859. (h) Gal'pern, M. G.; Luk'yanets, E. A. *Zh. Obshch. Khim.* **1969**, *39*, 2536−2541. (i) Kobayashi, N. In *Phthalocyanines, Properties and Applications*; Leznoff, C. C., Lever, A. B. P., Eds.; VCH: New York, 1993; Vol. 2, p 97. (j) Wang, C.; Bryce, M. R.; Batsanov, A. S.; Howard, J. A. K. *Chem. Eur. J.* **1997**, *3*, 1679−1690. (k) Kobayashi, N.; Ogata, H. *Eur. J. Inorg. Chem.* **2004**, 906−914.

(3) (a) Tadokoro, K.; Shoshi, M. (Ricoh Co., Ltd., Japan). Jpn. Kokai Tokkyo Koho JP 2000122316 A2 20000428, 2000; 22 pp. (b) Iijima, M.; Taho, F.; Yamazaki, K. (Fuji Xerox Co., Ltd., Japan). Jpn. Kokai Tokkyo Koho JP 10020529 A2 19980123, 1998; 10 pp; CODEN JKXXAF. (c) Hayashi, Y.; Sato, T. (Nippon Soda Co., Ltd., Japan). Jpn. Kokai Tokkyo Koho JP 04296762 A2 19921021, 1992; 4 pp. (d) Tadokoro, K.; Shoji, M.; Nanba, M. (Ricoh Co., Ltd., Japan). Jpn. Kokai Tokkyo Koho JP 11065142 A2 19990305, 1999; 24 pp. (e) Anayama, H.; Inai, K.; Miyazaki, H. (Canon K. K., Japan). Jpn. Kokai Tokkyo Koho JP 02035463 A2 19900206, 1990; 18 pp.

(4) Yamamoto, I.; Ota, K. (Eastern K. K., Japan). Jpn. Kokai Tokkyo Koho JP 02215783 A2 19900828, 1990; 3 pp.

(5) Tsai, C. W.; Chen, S. P.; Wen, T. C. *Chem. Phys.* **1999**, *240*, 191−196.

(6) (a) Shirk, J. S.; Pong, R. G. S.; Flom, S. R.; Heckmann, H.; Hanack, M. *J. Phys. Chem. A* **2000**, *104*, 1438−1449. (b) Perry, J. W.; Mansour, K.; Lee, I.-Y. S.; Wu. X.-L.; Bedworth, P. V.; Chen, C.-T.; Ng, D.; Marder, S. R.; Miles, P.; Wada, T.; Tian, M.; Sasabe, H. *Science* **1996**, *273*, 1533−1536. (c) Hanack, M.; Schneider, T.; Barthel, M.; Shirk, J. S.; Flom, S. R.; Pong, R. G. S. *Coord. Chem. Rev.* **2001**, *219*−*221*, 235. (d) Dini, D.; Yang, G. Y.; Hanack, M. *J. Chem. Phys.* **2003**, *119*, 4857−4864. (e) Cheng, W. D.; Wu, D. S.; Zhang, H.; Chen, J. T. *Phys. Rev. B* **2001**, *64*, 125109/1−11. (f) Vagin, S.; Barthel, M.; Dini, D.; Hanack, M. *Inorg. Chem.* **2003**, *42*, 2683−2694. (g) Barthel, M.; Dini, D.; Vagin, S.; Hanack, M. *Eur. J. Org. Chem.* **2002**, 3756−3762. (h) Henari, F.; Davey, A.; Blau, W.; Haisch, P.; Hanack, M. *J. Porphyrins Phthalocyanines* **1999**, *3*, 331−338. (i) De la Torre, G.; Vazquez, P.; Agullo-Lopez, F.; Torres, T. *Chem. Rev.* **2004**, *104*, 3723. (j) Coe, B. J. In *Comprehensive Coordination Chemistry II*; McCleverty, J. A., Meyer, T. J. Eds.; Elsevier: Oxford, U.K., 2004; pp 621−687.

(7) (a) Swarts, J. C.; Langner E. H. G.; Krokeide-Hoveb, N.; Cook, M. J. *J. Mater. Chem.* **2001**, *11*, 434−443. (b) Dini, D.; Hanack, M. In *The Porphyrin Handbook*; Kadish, K. M., Smith, K. M., Guilard, R., Eds.; Academic Press: Amsterdam, 2003; Vol. 17, pp 1−31. (c) Hanack, M.; Lang, M. *Adv. Mater.* **1994**, *6*, 819−833. (d) Schultz, H.; Lehmann, H.; Rein, M.; Hanack, M. *Struct. Bonding* **1990**; *74*, 41−146. (e) Berezin, B. D. *Coordination Compounds of the Porphyrins and Phthalocyanines*; Wiley: Chichester, U.K., 1981. (f) Lever A. B. P. *Adv. Inorg. Chem. Radiochem.* **1965**, *27*, 27−105.

(8) (a) Blake, I. M.; Anderson, H. L.; Beljonne, D.; Brédas, J. L.; Clegg, C. *J. Am. Chem. Soc.* **1998**, *120*, 10764−10765. (b) Ghosh, A. In *The Porphyrin Handbook, Theoretical and Physical Characterization*; Kadish, K. M., Smith, K. M., Guilard, R., Eds.; Academic Press: San Diego, CA, 2000; Vol. 7, pp 1−39. (c) Baerends, E. J.; Ricciardi, G.; Rosa, A.; van Gisbergen, S. J. A. *Coord. Chem. Rev.* **2002**, *230*, 5−27. (d) Delaere, D.; Tho Nguyen, M. *Chem. Phys. Lett.* **2003**, *376*, 329−337. (e) Cortina, H.; Senent, M. L.; Smeyers, Y. G. *J. Phys. Chem. A* **2003**, *107*, 8968−8974.

(9) (a) Enokida, T. *Jpn. J. Appl. Phys. Part 2 Lett.* **1992**, *31* (8A), L1135−L1136. (b) Lauter, U.; Schulze, M.; Wegner, G. *Macromol. Rapid Commun.* **1995**, *16*, 239−245. (c) Enokida, T.; Hirohashi, R.; Morohashi, N. *Bull. Chem. Soc. Jpn.* **1991**, *64*, 279−281. (d) Enokida, T.; Hirohashi, R. *Jpn. J. Appl. Phys. Part 2 Lett.* **1991**, *30* (4A), L768−L771.

(10) (a) Sheik-Bahae, M.; Said, A.A.; Wei, T. H.; Hagan, D. J.; Van Stryland E. W. *IEEE J. Quantum Electron.* **1990**, *26*, 760−769. (b) Wei, T. H.; Hagan, D. J.; Sence, M. J.; Van Stryland, E. W.; Perry, J. W.; Coulter, D. R. *Appl. Phys. B* **1992**, *54*, 46−51.

(11) (a) Egelhaaf, H. J.; Holder, E.; Herman, P.; Mayer, M. H.; Oelkrug, D.; Lindner, E. *J. Mater. Chem.* **2001**, *11*, 2445−2452. (b) Vincett, P. S.; Voigt, E. M.; Rieckhoff, K. E. *J. Chem. Phys.* **1971**, *55*, 4131−4140.

(12) (a) Ortí, E.; Brédas, J. L. In *Conjugated Polymeric Materials: Opportunities in Electronics, Optoelectronics and Molecular Electronics*; Brédas, J. L., Chance, R. R., Eds.; Kluwer Academic Publishers: Dordrecht, The Netherlands, 1990; pp 517−530. (b) Ortí, E.; Piqueras, M. C.; Crespo, R.; Brédas, J. L. *Chem. Mater.* **1990**, *2*, 110−116. (c) Ortí, E.; Brédas, J. L. *J. Chem. Phys.* **1990**, *92*, 1228−1235. (d) Ortí, E.; Brédas., J. L. *J. Am. Chem. Soc.* **1992**, *114*, 8669−8675.

(13) Becke, A. D. *Phys. Rev. A* **1988**, *38*, 3098−3100.

(14) Perdew, J. P. In *Electronic Structure of Solids*; Ziesche, P.; Eschrig, H., Eds.; Akademie Verlag: Berlin, 1991; pp 11−20.

(15) Becke, A. D. *J. Chem. Phys.* **1993**, *98*, 5648−5642.

(16) Kohn, W.; Sham, L. J. *Phys. Rev.* **1965**, *140*, A1133-A1136.

(17) Frisch, M. J.; Trucks, G. W.; Schlegel, H. B.; Scuseria, G. E.; Robb, M. A.; Cheeseman, J. R.; Zakrzewski, V. G.; Montgomery, J. A.; Stratmann, R. E.; Burant, J. C.; Dapprich, S.; Millam, J. M.; Daniels, A. D.; Kudin, K.; Strain, M. C.; Farkas, O.; Tomasi, J.; Barone, V.; Cossi, M.; Cammi, R.; Mennucci, B.; Pomelli, C.; Adamo, C.; Clifford, S.; Ochterski, J.; Petersson, J. A.; Ayala, P. Y.; Cui, Q.; Morokuma, K.; Salvador, P.; Dannenberg, J. J., Malick, D. K., Rabuck, A. D.; Raghavachari, K.; Foresman, J. B.; Cioslowski, J.; Ortiz, J. V.; Baboul, A. G.; Stefanov, B. B.; Liu, G.; Liashenko, A.; Piskorz, P.; Komaromi, I.; Gomperts, R.; Martin, R. L.; Fox, D. J.; Keith, T.; Al-Laham, M. A.; Peng, C. Y.; Nanayakkara, A.; Gonzalez, C.; Challacombe, M.; Gill, P. M. W.; Johnson, B. G.; Chen, W.; Wong, M. W.; Andres, J. L.; Head-Gordon, M.; Replogle, E. S.; Pople, J. A. *Gaussian 98* (Revision A.10); Gaussian, Inc.: Pittsburgh, PA, 1998.

(18) Yase, K.; Yasuoka, N.; Kobayashi, T.; Uyeda, N. *Acta Crystallogr., Sect. C* **1998**, *44*, 514−516.

(19) Brianso, J. L.; Regull, P.; Victori, L. *Afinidad* **1984**, *41*, 442−446.

(20) Ortí, E.; Crespo, R.; Piqueras, M. C.; Tomás, F. *J. Mater. Chem.* **1996**, *6*, 1751−1761.

(21) Zerner, M. C. In *Reviews in Computational Chemistry*; Lipkowitz, K. B., Boyd, D. B., Eds.; VCH: New York, 1991; pp 313−366.

(22) Zerner, M. C.; Loew, G. H.; Kichner, R.; Mueller-Westerhoff, U. T. *J. Am. Chem. Soc.* **1980**, *102*, 589−599.

(23) Beljonne, D.; O'Keefe, G. E.; Hamer, P. J.; Friend, R. H.; Anderson, H. L.; Brédas, J. L. *J. Chem. Phys.* **1997**, *106*, 9439−9460.

(24) Dini, D.; Martin, R. E.; Holmes, A. B. *Adv. Funct. Mater.* **2002**, *12*, 299−306.

(25) Lüer, L.; Egelhaaf, H. J.; Oelkrug, D. *Opt. Mater.* **1998**, *9*, 454−460.

(26) (a) Winter, G.; Heckmann, H.; Haisch, P.; Eberhardt, W.; Hanack, M.; Luer, L.; Egelhaaf, H. J.; Oelkrug D. *J. Am. Chem. Soc.* **1998**, *120*, 11663−11673. (b) Haisch, P.; Winter, G.; Hanack, M.; Lüer, L.; Egelhaaf, H. J.; Oelkrug, D. *Adv. Mater.* **1997**, *4*, 316−321.

(27) (a) Lever, A. B. P.; Pickens, S. R.; Minor, P. C.; Licoccia, S.; Ramaswamy, B. S.; Magnell, K. *J. Am. Chem. Soc.* **1981**, *103*, 6800−6806. (b) Orti, E.; Piqueras, M. C.; Crespo, R.; Bredas, J. L. *Chem. Mater.* **1990**, *2*, 110−116.

(28) (a) Dhami, S.; De Mello, A. J.; Rumbles, G.; Bishop, S. M.; Phillips, D.; Beeby, A. *Photochem. Photobiol.* **1995**, *61*, 341−346. (b) Hush, N. S.; Woolsey, I. S. *Mol. Phys.* **1971**, *21*, 465−474. (c) Kobayashi, N.; Lever, A. B. P. *J. Am. Chem. Soc.* **1987**, *109*, 7433−7441. (d) Pelliccioli, A. P.; Henbest, K.; Kwag, G.; Carvagno, T. R.; Kenney, M. E.; Rodgers, M. A. J. *J. Phys. Chem. A* **2001**, *105*, 1757−1766.

(29) Hempstead, M. R.; Lever, A. B. P.; Leznoff, C. C. *Can. J. Chem.* **1987**, *65*, 2677.

(30) (a) Schomaker, V.; Pauling, L. *J. Am. Chem. Soc.* **1939**, *61* (1), 1769−1780. (b) Brown, R. D.; Coller, B. A. W. *Theor. Chim. Acta* **1967**, *7*, 259−282. (c) Lowdin, P. O. *J. Chem. Phys.* **1951**, *19*, 1323−1324.

(31) (a) Sakakibara, Y.; Vacha, M.; Tani, T. *Mol. Cryst. Liq. Cryst.* **1998**, *314*, 71−76. (b) Spaeth, M. L.; Sooy, W. R. *J. Chem. Phys.* **1998**, *48*, 2315−2323. (c) Farren, C.; Fitzgerald, S.; Beeby, A.; Bryce, R. M. *Chem. Commun.* **2002**, 572−573. (d) Eastwood, D.; Edwards, L.; Gouterman, M.; Steinfeld, J. *J. Mol. Spectrosc.* **1966**, *20*, 381−390.

(32) (a) Yoon, M.; Cheon, Y.; Kim, D. *Photochem. Photobiol.* **1993**, *58*, 31−36. (b) Huang, T. H.; Sharp, J. H. *Chem. Phys.* **1982**, *65*, 205−216.

(33) Pascal, L.; Vanden Eynde, J. J.; Van Haverbeke, Y.; Dubois P.; Michel, A.; Rant U.; Zojer, E.; Leising, G.; Van Dorn L. O.; Gruhn, N. E.; Cornil, J.; Bredas, J. L. *J. Phys. Chem. B* **2002**, *106*, 6442−6450.

(34) (a) Mack, J.; Stillman, M. J. *J. Porphyrins Phthalocyanines* **2001**, *5*, 67−76. (b) Mack, J.; Stillman, M. J. *Coord. Chem. Rev.* **2001**, *219−221*, 993−1032. (c) Stillman, M. J.; Nyokong, T. In *Phthalocyanines, Properties and Applications*; Leznoff, C. C., Lever, A. B. P., Eds.; VCH: New York, 1989; Vol. 1, p 133−257.

(35) Goutermann, M. In *The Porphyrins*; Dolphin, R., Ed.; Academic Press: New York, 1977; Vol. 3, pp 1−157.

(36) Aranda, F. J.; Rao, D. Narayana; Rao, D. V. G. L. N.; Nakashima, M.; De Cristofano, B. *Proc. SPIE* **1996**, *2853*, 180−189.

(37) Turro, N. J. *Modern Molecular Photochemistry*; Benjamin Cummings; Menlo Park, CA, 1978.

(38) Mansour, K.; Alvarez, D., Jr.; Perry, K. J.; Choong, I.; Marder, S. R.; Perry, J. W. *SPIE Proc.* **1993**, *1853*, 132−141.

(39) Sun, W.; Wu, Z. X.; Yang, Q. Z.; Wu, L. Z.; Tung, C. H. *Appl. Phys. Lett.* **2003**, *82*, 850−852.

(40) (a) Blau, W.; Byrne, H.; Dennis, W. M.; Kelly, J. M. *Opt. Commun.* **1985**, *56*, 25. (b) Sanghadasa, M.; Shin, I. S.; Clark, R. D.; Guo, H.; Penn, B. G. *J. Appl. Phys.* **2001**, *90*, 31.

(41) (a) Jaffe, H. H.; Orchin, M. *Theory and Application of Ultraviolet Spectroscopy*; Wiley: New York, 1962. (b) Ricciardi, G.; Rosa, A.; Baerends, E. J. *J. Phys. Chem. A* **2001**, *105*, 5242. (c) Baerends, E. J.; Ricciardi, G.; Rosa, A.; Van Gisbergen, S. J. A. *Coord. Chem. Rev.* **2002**, *230*, 5. (d) Ricciardi, G.; Rosa, A.; Van Gisbergen, S. J. A.; Baerends, E. J. *J. Phys. Chem. A* **2000**, *104*, 635.

(42) (a) Yang, G. Y.; Hanack, M.; Lee, Y. W.; Chen, Y.; Lee, M. K. Y.; Dini, D. *Chem. Eur. J.* **2003**, *9*, 2758−2762. (b) Dini, D.; Barthel, M.; Schneider, T.; Ottmar, M.; Hanack, M. *Solid State Ionics* **2003**, *165*, 289−303.

(43) (a) Hiller, W.; Straehle, J.; Kobel, W.; Hanack, M. *Z. Kristallogr.* **1982**, *159*, 173−183. (b) Yamaguchi, S.; Sasaki, Y. *Chem. Phys. Lett.* **2000**, *323*, 35−42. (c) Saito, T.; Sisk, W.; Kobayashi, T.; Suzuki, S.; Iwayanagi, T. *J. Phys. Chem.* **1993**, *97*, 8026−8031. (d) Popovic, Z. D.; Hor, A. M. *Mol. Cryst. Liq. Cryst.***1993**, *228*, 75−80. (e) Mizuguchi, J.; Rihs, G.; Karfunkel, H. R. *J. Phys. Chem.* **1995**, *99*, 16217−16227. (f) Gulbinas, V. *Chem. Phys.* **2000,** *261*, 469−479. (g) Law, K. Y. *Chem. Rev.* **1993**, *93*, 449−486.

(44) (a) Gould, R. D. *Coord. Chem. Rev.* **1996**, *156*, 237−274. (b) Meier, H.; Albrecht, W.; Tschirwitz, U. *Angew. Chem., Int. Ed. Engl.* **1972**, *11*, 1051−1061.

(45) (a) Day, P.; Price, M. G. *J. Chem. Soc. A* **1969**, 236−240. (b) Day, P.; Williams, R. J. P. *J. Chem. Phys.* **1965**, *42*, 4049−4050. (c) Dahlberg, S. C.; Musser, M. E. *J. Chem. Phys.* **1980**, *72*, 6706−6711. (d) Mizuguchi, J. *Jpn. J. Appl. Phys.* **1981**, *20*, 2073−2078. (e) Harrison, S. E. *J. Chem. Phys.* **1969**, *50*, 4739−4742. (e) Law, K. Y. *Chem. Rev.* **1993**, *93*, 449−486.

(46) Noolandi, J.; Hong, K. M. *J. Chem. Phys.* **1979**, *70*, 3230−3236.

(47) Gutmann, F.; Lyons, L. E. *Organic Semiconductors*; Wiley: New York, 1967.